



Nonlinear Interaction of Optimal Streaks and Tollmien-Schlichting Waves

SHERVIN BAGHERI

Shervin Bagheri

Nonlinear Interaction of Optimal Streaks and Tollmien-Schlichting Waves

Contents

1	Introduction	1
1.1	Background	1
1.2	Previous Work	3
1.3	Aim of the Thesis	4
2	General Formulation	7
2.1	Governing Equations	7
2.2	Mean Flow	9
2.3	Perturbations	10
3	Numerical Procedure	15
3.1	Streaks with PSE Scalings	15
3.2	Removal of the Step-size Restriction for nonlinear PSE	16
3.3	A Comparison to DNS	17
4	Results	21
4.1	The Mean Flow in the Presence of Streaks	21
4.2	Characteristics of the Streaks Investigated	22
4.3	The Stabilizing Effect of the Streak Amplitude	26
4.4	The Stabilizing Effect of the Spanwise Wave Number of the Streak	27
4.5	The Effect of Pressure Gradients on Streaks	32
4.6	Conclusions	33
5	Discussion	35
A	PSE Matrices	37
	Bibliography	39

1 Introduction

1.1 Background

Stability and Transition

One of the great classical challenges in physics, remaining yet today, is the question of why flows become turbulent. Hydrodynamic stability is the study of the transition of a flow from a stable laminar state to a turbulent and chaotic state. Generally, one is interested in the response of a laminar basic flow to a perturbation. The grow and decay of the perturbation determines the stability of the flow. A natural extension of these studies are the attempts to control the flow by the delay of transition of a laminar flow or by “laminarizing” a turbulent flow. This is called *flow control* and have many engineering applications such as the design of vehicles and aircraft wings. The disadvantage of turbulence in flows is mainly energy losses and the main objective in applications is to reduce drag by the delay of transition, in order to minimize the fuel consumption or to increase the speed.

The transition to turbulence is often complicated and can follow many possible routes. Therefore, it is often divided into different stages. One of the first stages is the study of the linear growth of disturbances superposed on a basic flow (also called the mean flow). Roughly speaking, there are two classical methods of investigation at this stage. The first method, sometimes called the *energy method*, consists of calculating the evolution of the kinetic energy of a disturbance in time. Conclusions are drawn depending on whether the energy decreases or increases with time. The second method analyzes the manner in which disturbances develop in the flow by solving the appropriate differential equations, often consisting of the Navier-Stokes equations or a set of disturbance equations. If the disturbances grow in time or space the basic flow is unstable. When the disturbances reach a finite amplitude nonlinear effects become important. The next stage of transition is when the finite amplitude disturbance saturates and the flow transforms into a new state. Only in a few transition scenarios does the primary instability directly cause turbulence. Instead, the new flow state becomes a more complicated basic flow on which *secondary instabilities* can grow. The final stage is the breakdown where nonlinearities excite an increasing number of scales and frequencies of the flow.

Two basic scenarios are transitions emanating from exponential instabilities and those that do not, the so called bypass transitions. Basically, these scenarios can be attributed to two primary growth mechanisms. They are the exponential growth associated with inflectional instabilities and the transient growth associated with the lift-up effect. These concepts are introduced in this work. There are numerous methods of preventing transition to turbulence in a flow and the most common one is to change the basic flow. This can be done for instance by enforcing favorable pressure gradients or by wall suction, i.e. forcing a part of a flow through a porous boundary.

It has been found by recent numerical and experimental studies that by

generating a particular type of transient growth called *streaks*, the mean flow in flat-plate boundary layers, can be stabilized for disturbances of exponential type. This work aims at performing numerical simulations of the observed stabilization effect of streaks on exponential instabilities in boundary-layer flows. The purpose is to characterize and understand the nonlinear interaction of these disturbances with each other and with the mean flow. The numerical method is based on a parabolized approximation of the disturbance equations called Parabolized Stability Equations. It provides a much more feasible numerical task than the full Navier-Stokes and with a very good accuracy. The results obtained from this work will provide valuable information for a further development of laminar-turbulent transition delay by means of streaks. A very brief background of the disturbances used in this work is given in order to understand the fundamental results, the reader is addressed to the book by Schmid and Henningson [19] for a complete coverage of the subject.

Exponential Growth

For disturbance of exponential character with low amplitudes one can assume a parallel mean flow and only wave-like solutions (also referred to as modes) in order to derive a coupled complex eigenvalue problem from the linearized disturbance equations. Classical linear stability theory involves solving this eigenvalue problem, called the Orr-Sommerfeld and Squire equations and analyzing the evolution of the eigensolutions. This kind of Fourier decomposition of the solutions allows two different approaches to study the evolution of disturbances, namely in time space or in spatial space. Temporal stabilities is a much easier mathematical task to consider as the eigenvalue problem of Orr-Sommerfeld is then of the order two, whereas the problem of determining the spatial stability the eigenvalue appears nonlinearly up to the fourth order. However, almost every physical situation requires the modeling of the disturbance amplitude or energy as spatially growing modes. For instance, this allows us to study non-parallel mean flows and harmonic point sources.

Lord Rayleigh stated in 1880 the inflection point theorem from studying the inviscid form of the Orr-Sommerfeld equation. This theorem relates the existence of an unstable mode to the occurrence of an inflection point in the mean flow, i.e when the second derivate of the mean flow changes sign. Later, Fjortoft in 1950 improved the criterion for instability by stating that the inflection point has to be a maximum of the spanwise mean vorticity. Both of these theorems constitute necessary but not sufficient requirements for inviscid flows to become unstable. However, it had been observed that pipe flow was unstable, despite the fact of a missing inflection point in the mean profile, so one must conclude that viscosity is in this case destabilizing. The viscous unstable mode with the largest growth rate is called a Tollmien-Schlichting wave (TS wave) in honor of the researches (Tollmien, 1935; Schlichting, 1933) who first showed that the Orr-Sommerfeld equation has unstable solutions for flows without inflection points.

Squire in 1933 and Gaster in 1962 made important contributions to linear stability theory. Squire discovered that two-dimensional waves are the first to become unstable in incompressible boundary-layer flows. As a consequence most of the early work on stability concerned only two-dimensional waves. Gaster's transformation gives a relation between the disturbance growth rates obtained by temporal analysis and growth rates from spatial analysis.

Algebraic Growth

The total sum of modes, which individually are stable and therefore decrease with time or in space, can generate growth and eventually lead to turbulence. Mathematically this is because the linear operator representing the coupled Orr-Sommerfeld and Squire equations is non-normal and consequently have non-orthogonal eigenfunctions. The discovery of this transition scenario, began with an observation made by Ellingsen and Palm in 1975. They found that in the inviscid temporal case the growth of a perturbation is linear with time. This type of growth is called algebraic instability. The investigation by Gustavsson in 1991 showed however, that viscosity will set a limit on the temporal growth, and after a certain time the growth will decay. Hence this type of growth is also referred to as transient growth.

The importance of transient growth in transition to turbulence was pioneered by Luchini in 1996, who considered the spatial case in a growing boundary layer. His results indicated that algebraic growth not always is followed by a viscous decay and therefore concluded that non-modal growth may be important for boundary layer transition. As a consequence of Luchini's observation there have been numerous numerical and experimental studies of the role of transient growth in non-modal transition. It has been discovered that the traditional TS wave dominated transition scenario is bypassed by the transition caused by transient growth. This means that transition to turbulence takes place below the critical Reynolds number predicted by classical theory. For this reason this transition scenario is called bypass transition.

The physical mechanism behind transient growth is called the lift-up effect and was first explained by Landahl in 1995. He argued that a fluid element near the shear wall initially retains its horizontal momentum in the wall-normal direction, hence causing a streamwise disturbance. It had been known that for the Blasius boundary layer, free-stream turbulence (FST) induces disturbances into the boundary layer which give rise to streamwise oriented structures of low and high speed fluid which generate spanwise modulations of the boundary layer thickness. These *streaky* structures was first observed by Klebanoff in 1971 and are therefore called Klebanoff modes or streaks.

In transitional studies one is often interested to generate a disturbance that experiences maximum growth with minimum energy input. Butler and Farrell found in 1992 that the optimal perturbations used as initial conditions which maximize the energy growth downstream consists of streamwise vortices that develop into streaks downstream. Andersson *et al.*[16] later calculated the optimal disturbances in a growing boundary layer and discovered that optimally growing streaks are remarkably similar to streaks generated experimentally by free stream turbulence.

1.2 Previous Work

Only recently has computer power become sufficient and numerical methods developed efficient enough to enable nonlinear calculations of the interaction of TS waves and streaks. Therefore, the early studies are mostly experimental and mainly focused on the importance of TS waves for transition to turbulence caused by free stream turbulence. In these studies, the stabilizing effect of streaks on TS waves was discovered by "accident". In the more recent numerical and experimental work a different approach has been adopted, directly aimed at the study of the stabilization of TS by the use of streaks in order to delay transition. The investigations are done by considering the TS wave as a secondary instability growing on a streaky boundary layer.

Spanwise modulations of flat-plate boundary thickness caused by streaks

result in new more complicated flow (called streaky boundary layers) and have received much attention. The streaky boundary layer can support both inviscid and viscous growth of disturbances. Andersson *et al.*[17] showed by numerical simulation that in streaky boundary layers the mean flow can develop an inflection point so that inviscid growth leads to breakdown and transition to turbulence. The inviscid stability of the streaky boundary layer depends on the amplitude of the streak, where the critical amplitude for this particular streak is 26% of the free-stream velocity. The viscous stability of streaky boundary layers has resulted in numerous experimental studies of the development of TS waves in the presence of streaks. Besides from the observation that transition of streaky flows is significantly promoted by TS waves (see Westing *et al.*[2] and references therein), these experiments also reveal the following:

1. In the presence of streaks the TS wave is 3D. For low amplitudes the TS wave do not amplify as it does in the absence of a streak.
2. The decrease in the growth of TS waves is attributed to the stabilizing role of the mean flow distortion induced by the streaks.

These two observations are fundamental in this thesis. With the first observation, the idea of using streaks to stabilize TS waves and eventually delay transition to turbulence initiated numerical studies by Brandt and Cossu [9]. They showed by temporal and spatial numerical simulations that optimal streaks are able to stabilize low-amplitude TS waves in a flat-plate boundary layer. They also found that the damping of TS waves increases with the streak amplitude. These observations were confirmed in an experimental study by Fransson *et al.*[12] specifically aimed at stabilizing TS waves by the generation of streaks with roughness elements close to the leading edge. Recently [13], they also showed that the presence of streaks can delay TS dominated transition to turbulence. In an another article by Brandt and Cossu [11] the linear viscous stability of the streaky boundary layer was analyzed. By using the energy method, they showed that the physical mechanism behind the stabilizing effect of streaks is the spanwise shear of the modulated mean flow. The streak amplitude was shown to increase the total energy dissipation of the TS wave, thereby reducing the growth rate and eventually leading to stability.

1.3 Aim of the Thesis

In transition scenarios caused by exponential disturbances, the transition method relies on the reduction of exponential growth in the linear regime. The use of streaks might develop a new transition method of this kind, where the streak amplitude plays an important role in stabilizing exponential growth. There are however some concerns regarding the streak amplitude. As mentioned previously, the maximum streak amplitude appears to be limited by the occurrence of secondary inflectional instabilities on the streak. With the largest streak amplitude (close to the limit 26%) used in the calculations of Brandt and Cossu, they were able to delay the onset of instability up to Reynolds number 850. It is not clear if streak amplitudes below the inviscid instability limit are large enough to stabilize TS waves whose unstable region is further downstream. There exists also a “practical” issue concerning the streak amplitude, which is the lack of a experimental scheme for generating streaks with high amplitudes. In the recent experiments by Fransson *et al.*[12, 13] where roughness elements have been used to generate the optimal streaks, streak amplitudes cannot reach greater values than a few percent ($\sim 5\%$) of the free-stream velocity. For larger amplitudes a vortex shedding instability develops behind the roughness elements.

Therefore, it is important and one of the aims of the present study to investigate and optimize other streak parameters in order to achieve stabilization for a wider range of TS waves and larger Reynolds numbers. This could increase the performance of a possible streak-based transition delay method. The recent numerical investigations [9, 11] by Brandt and Cossu [9] are based on four optimal streaks with different amplitudes, but originating from a single optimal perturbation, i.e. initial conditions. No attempts have been made to optimize the streak.

The investigation of Brandt and Cossu [9, 11] is mainly focused on the temporal growth of TS waves. To allow for a quantitative comparison with other transition delay methods, the computation of spatial growth rates is necessary, i.e. in the N-factors in the e^N method. But this is an overwhelming task even for fast computers if one wants to solve the full Navier-Stokes (DNS). The viability of such a task requires a less computational demanding effort, such as solving the nonlinear Parabolized Stability Equations (PSE). It is also the objective of this thesis to use the PSE approximation to study the interaction of streaks and TS waves. This is not a trivial task, as the PSE are designed to study exponential growth. Therefore, additional terms of higher order than the PSE approximation needs be accounted for in order to calculate the algebraic growth of streaks.

Below follows a summary of the objectives of the present investigation:

1. To confirm the stabilization effect using Parabolized Stability Equations and compare the obtained result with the DNS-simulations of Brandt and Cossu [9].
2. To perform parametric studies of the amplitude and spanwise wave number of streaks against the spatial growth of TS waves of different frequencies.
3. To characterize the mean flow in the presence of streaks and investigate its stabilizing effect.

2 General Formulation

2.1 Governing Equations

Nonlinear Disturbance Equations

The fundamental equations of Naviers-Stokes are the cornerstone in every field of fluid mechanics, and even so in deriving the equations describing the evolution of a disturbance in a stable laminar flow. The equations of Navier-Stokes describe the evolution of a viscous flow in space and with time and consist of the conservation laws for momentum and mass. For an incompressible flow, the equations are

$$\begin{aligned} \frac{\partial \mathbf{u}}{\partial t} + \nabla p - \frac{1}{\text{Re}} \nabla^2 \mathbf{u} &= -(\mathbf{u} \cdot \nabla) \mathbf{u} \\ \nabla \cdot \mathbf{u} &= 0, \end{aligned} \quad (2.1)$$

where $\mathbf{u}(\mathbf{x}, t) = (u, v, w)$ is the velocity vector and p is the pressure. The streamwise, wall-normal and spanwise velocity components of the flow are denoted as u , v and w respectively. Furthermore, x represents the streamwise, y the wall-normal and z the spanwise coordinate. For boundary-layer flows, the equations are non-dimensionalized by the free-stream velocity U_∞ , a length scale L and the kinematic viscosity ν of the flow, which together defines the Reynolds number as, $\text{Re} = \frac{U_\infty L}{\nu}$. The boundary and initial conditions are $\mathbf{u}(0, t) = 0$ on solid boundaries and $\mathbf{u}(\mathbf{x}, 0) = \mathbf{u}^0(\mathbf{x})$ respectively.

The disturbance equations are derived from equation (2.1) by considering a basic flow (U, V, W, P) and a pertubated flow $(U + u', V + v', W + w', P + p')$ both satisfying equation (2.1). By subtracting the equations for the basic flow and the pertubated flow, the nonlinear disturbance equations (omitting the primes) are found to be

$$\begin{aligned} \frac{\partial \mathbf{u}}{\partial t} + \nabla p - \frac{1}{\text{Re}} \nabla^2 \mathbf{u} + (\mathbf{U} \cdot \nabla) \mathbf{u} + (\mathbf{u} \cdot \nabla) \mathbf{U} &= -(\mathbf{u} \cdot \nabla) \mathbf{u} \\ \nabla \cdot \mathbf{u} &= 0. \end{aligned} \quad (2.2)$$

Together with the boundary condition $\mathbf{u}(0, t) = 0$ on solid boundaries and the initial condition $\mathbf{u}(\mathbf{x}, 0) = \mathbf{u}^0(\mathbf{x})$, they govern the development of a disturbance on a laminar basic flow.

The Nonlinear Parabolized Stability Equations

To correctly account for downstream development of disturbances a spatial technique is necessary, but it is a formidable computational task to solve the Navier-Stokes equations (2.1) (called Direct Navier-Stokes or DNS). In the beginning of the last century a new technique was developed to solve the stability equations (2.2) for disturbances associated with exponential growth by Herbert and Bertolotti [5, 20]. It is based on a few simple assumption that reduce the ellipticity of (2.2) and provide a much more feasible numerical task with a very good accuracy. One of the characteristics of elliptic differential equations is

dependency of the solutions on the initial conditions, i.e. the elliptical terms in equation (2.2) propagate information upstreams. By an appropriate scaling of the variables the elliptical terms can be neglected and we can march in space with initial conditions that are independent of the upstream history. In this way a set of nearly parabolized stability equations (PSE) are derived. PSE have one remaining elliptic term, and as a consequence the method is numerically unstable for a certain limit on the spatial step size [18].

First, we assume a stability problem, where the mean flow is steady and two-dimensional and the disturbances are homogeneous in the spanwise direction and periodic in time. The general form of the mean flow is

$$\mathbf{U} = (U(x, y), V(x, y), 0) \quad (2.3)$$

and the Fourier transform of disturbances (denoted as \mathbf{q} instead of \mathbf{u}) give,

$$\mathbf{q}(x, y, z, t) = \sum_{n=-\infty}^{\infty} \sum_{m=-\infty}^{\infty} \tilde{\mathbf{q}}_{mn}(x, y) e^{i(m\beta_0 z - n\omega_0 t)}. \quad (2.4)$$

Here, $U(x, y), V(x, y)$ are the streamwise and wall-normal components of the mean flow, $\tilde{\mathbf{q}}_{mn} = (\tilde{u}_{mn}, \tilde{v}_{mn}, \tilde{w}_{mn}, \tilde{p}_{mn})$ is the amplitude function for the mode $(m\beta_0, n\omega_0)$ (referred to as (m, n)), where β_0 denotes the wave number in the spanwise direction and ω_0 the frequency of the disturbance. In the spatial framework of disturbance growth, β_0 and ω_0 are real valued. The Reynolds number used throughout this work is defined as $R_0 = U_\infty \delta_0 / \nu$, where $\delta_0 = \sqrt{\nu x_0^* / U_\infty}$ is a fix boundary layer parameter and x_0^* is the dimensional streamwise location of the leading edge in the flat plate boundary-layer.

Second, two fundamental assumptions are required to derive the PSE:

1. The streamwise component of the disturbance amplitude for each mode (m, n) in (2.4) consists of an oscillatory part and an amplitude part,

$$\tilde{\mathbf{q}}_{mn} = \hat{\mathbf{q}}_{mn}(x, y) e^{i \int_{x_0}^{x_1} \alpha_{mn}(x') dx'} \quad (2.5)$$

where α_{mn} is the complex streamwise wave number.

2. a) The disturbance amplitude $\hat{\mathbf{q}}_{mn}(x, y)$ varies slowly in the streamwise direction, whereas the exponential part of (2.5) varies fast. This is formulated by introducing X as the weak variation in x -direction and $1/R_0$ (assuming R_0) as the scale separation, i.e.

$$X = \frac{x}{R_0} \quad \frac{\partial}{\partial x} \sim \frac{1}{R_0}. \quad (2.6)$$

- b) The wall-normal component of the mean flow is small. Using the same scale parameter as above we can write,

$$V \sim \frac{1}{R_0}. \quad (2.7)$$

The disturbance in its general form becomes

$$\mathbf{q}_{mn} = \hat{\mathbf{q}}_{mn}(X, y) e^{i(\int_{x_0}^{x_1} \alpha_{mn}(X') dx' + m\beta_0 z - n\omega_0 t)}. \quad (2.8)$$

Inserting the perturbation (2.8) into the nonlinear disturbance equations (2.2) and neglecting all terms $\mathcal{O}(1/R_0^2)$ and higher, a set of nearly parabolic partial differential equations is obtained,

$$A \hat{\mathbf{q}}_{mn} + B \frac{\partial \hat{\mathbf{q}}_{mn}}{\partial y} + C \frac{\partial^2 \hat{\mathbf{q}}_{mn}}{\partial y^2} + D \frac{\partial \hat{\mathbf{q}}_{mn}}{\partial x} = \mathbf{f}_{mn} \quad (2.9)$$

$$\hat{\mathbf{q}}_{mn} = 0 \quad \text{on solid boundaries.}$$

A, B, C, D and f_{mn} are functions of $\alpha_{mn}, \beta_0, \omega_0$ and of the mean flow \mathbf{U} . The term \mathbf{f}_{mn} is the Fourier component of the nonlinear terms. These functions can be found in Appendix A. For nonlinear equations such as (2.9), the Fourier components do not evolve independently as in the linear case, but are coupled together. The total forcing,

$$\mathbf{F} = \sum_{n=-\infty}^{\infty} \sum_{m=-\infty}^{\infty} \mathbf{f}_{mn}(x, y) e^{i(\int_{x_0}^{x_1} \alpha_{mn}(x') dx' + m\beta_0 z - n\omega_0 t)}, \quad (2.10)$$

causes nonlinear interaction of modes with larger amplitude than a predefined threshold, which results in the excitation of a new modes [19]. Thus, the nonlinear terms are responsible for the propagation of energy from one mode to another.

The stability of the disturbed flow $\mathbf{U} + \mathbf{q}$ in space, depends on both the amplitude function $\hat{\mathbf{q}}_{mn}(x, y)$ and the streamwise wavelength $\alpha_{mn}(x)$. As both the amplitude and exponential function depend on streamwise variable x , one more equation is required in order to ensure that most x -variation of the disturbance will be accounted for by the exponential function. Therefore, the normalization condition is introduced,

$$\int_0^{y_{max}} \hat{\mathbf{q}}_{mn}^* \frac{\partial \hat{\mathbf{q}}_{mn}}{\partial x} dy, \quad (2.11)$$

where $\hat{\mathbf{q}}_{mn}^*$ is the complex conjugate of $\hat{\mathbf{q}}_{mn}$.

2.2 Mean Flow

The mean flows considered are two-dimensional over a flat plate and solutions to the boundary-layer equations, which are a linear parabolic approximation of the Navier-Stokes (2.1). The reader is referred to Schlichting[7] for a comprehensive theory on boundary layers. A boundary layer over a flat plate grows as $\delta \sim \sqrt{\nu}$, where δ is the boundary layer thickness [7] (see Figure 2.1). The fundamental assumption is that the boundary layer thickness is very small compared to specified length scale of the flat plate, i.e. $\delta \ll L$. Furthermore, we assume that the flow in the wall-normal direction varies slowly compared to the streamwise direction. Thus, the following scalings are introduced,

$$V \sim \delta, \quad y \sim \delta, \quad U \sim L, \quad x \sim L. \quad (2.12)$$

With these scalings applied to the linear left-hand side of equation (2.1) and terms of $\mathcal{O}(1/R)$ and higher neglected, a set of differential equations that do not contain the Reynolds number are obtained. As a consequence the solutions belong to a set called *similarity solutions*, i.e. the velocity profiles at different streamwise locations are similar and by a coordinate transformation the equations can be reduced to one ordinary differential equation [7].

The velocity profiles formulated by similarity variables are of the form,

$$-U_{\infty}(x) = Cx^m, \quad (2.13)$$

where C and m are constants. The free-stream velocity $U_{\infty}(x)$ is related to a free-stream mean pressure gradient as,

$$\frac{dP_{\infty}}{dx} = -U_{\infty} \frac{dU_{\infty}}{dx}. \quad (2.14)$$

Introducing the similarity variable as,

$$\eta = y \sqrt{\frac{m+1}{2} \frac{U_{\infty}}{\nu x}} \quad (2.15)$$

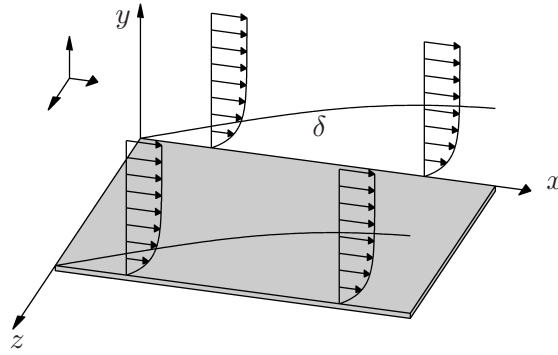


Figure 2.1: The flat-plate boundary layer.

and representing the velocity components in the boundary layer equations as stream functions [7, 19], a nonlinear ordinary differential equation is derived,

$$\begin{aligned} f''' + ff' + \beta_H(1 - f'^2) &= 0 \\ f(0) = f'(0) &= 0, \quad f'(\infty) = 1, \end{aligned} \quad (2.16)$$

where $f(\eta)$ is the stream function and the prime denotes derivatives with respect to the similarity variable η . The Hartree parameter β_H is related to m by

$$\beta_H = \frac{2m}{m+1}.$$

The Hartree parameter is a measure of the acceleration or deceleration of the free-stream. For the Blasius boundary layer the parameter is $\beta_H = 0$, for favorable pressure gradient $\beta_H > 0$ and for adverse pressure gradient $\beta_H < 0$. In the case of favorable pressure gradients the mean velocity appears fuller than the Blasius velocity profile resulting in a more stable boundary layer for exponentially growing perturbations. For the case of adverse pressure gradient the mean flow reveals points of inflection.

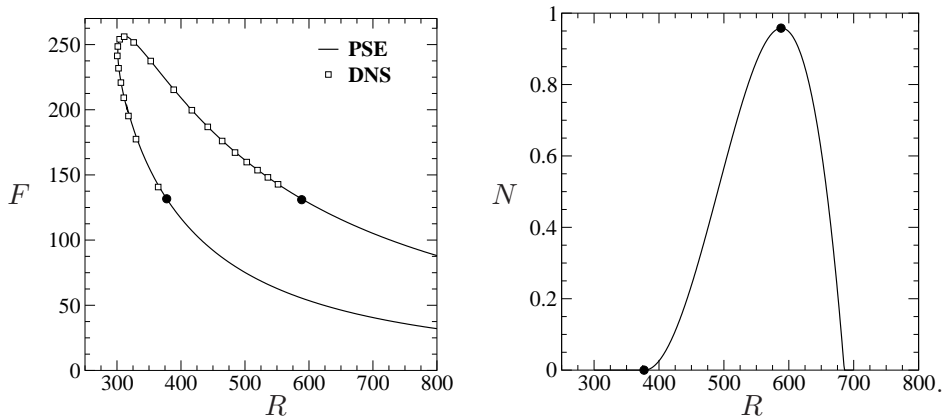
2.3 Perturbations

Tollmien-Schlichting Waves

A TS wave is an unstable mode of the Orr-Sommerfeld equation, arising from the viscosity of the flow. Squires theorem states that in an incompressible flow the two-dimensional TS wave is the most unstable wave. Thus, the perturbations considered in flat-plate boundary layer flow is of the form (2.5) with zero spanwise wave number,

$$\mathbf{q}_n = \hat{\mathbf{q}}_n(x, y) e^{i \int_{x_0}^{x_1} \alpha_n(x') dx' - in\omega_0 t}. \quad (2.17)$$

The exponential stability problem consists of solving the equation (2.9) for the disturbance of the form (2.17). The base flow \mathbf{U} is obtained from the Blasius solution. The initial values of ω_0 and $\mathbf{q}_n(t = t_0)$ is given at a streamwise station R_0 . For each downstream station $R_i \in [R_0, R_1]$ and mode $(0, n)$, the streamwise wave number $\alpha_n \in \mathbb{C}$ is obtained by satisfying iteratively the normalization condition (2.11). For $\alpha_i > 0$ the disturbance grows exponentially in the mean flow. During this iterative process, the forcing terms (2.10) are calculated iteratively as well, and new modes with amplitudes larger than a threshold are generated.



(a) The neutral stability curve for a Blasius boundary layer calculated with PSE and DNS.

(b) Linear growth of TS wave of $F = 131$.

Figure 2.2: TS wave with a sufficiently small amplitude to allow the nonlinear terms to be neglected. According the neutral stability curve (a) Branch I is approximately at $R_0 = 378$ and branch II at $R_0 = 589$, which is good agreement of with the location of growth and decay of the disturbance (b)(marked by black dots).

To specify the time periodicity of the disturbance, a non-dimensional frequency is defined as

$$F = \frac{\omega}{R} 10^6. \quad (2.18)$$

Figure 2.2 is a *neutral stability curve* for a Blasius boundary layer. The curve defines the boundary between areas in frequency and spatial space where unstable modes are present. The left boundary defines the lowest Reynolds number for which an unstable mode exists and is referred to as Branch I. After crossing the boundary the unstable mode begins to grow until Branch II is reached, were it once again begins to decay.

To describe the development of an initial perturbation a measure of its size it is necessary and several different definitions can be found in the literature, see Fasel *et al.*[6]. In this work, the kinetic energy of the TS wave is frequently used as a measurement of the growth,

$$e_k = \frac{1}{2} \int_0^{y_{max}} \mathbf{q} \cdot \mathbf{q}^* dy. \quad (2.19)$$

Two other convenient forms of growth measurements are the relative amplification of a disturbance called the *N-factor* and the maximum growth rate α_i^* . They are defined as

$$N = \ln \left(\frac{E(x_1)}{E(x_2)} \right) \quad \text{and} \quad \alpha_i^* = \max_{x \in [x_0, x_1]} \alpha_i, \quad (2.20)$$

where x_1 and x_2 are streamwise locations of Branch I and II of the neutral stability curve, respectively. Figure 2.2 shows a neutral curve and the linear growth of a TS wave in Blasius boundary layer to illustrate the concepts introduced.

Optimal Disturbances and Streaks

Streaks arise when flat-plate boundary layers are subjected to high levels of free-stream turbulence. These disturbances are known to be elongated in the

streamwise direction, to appear with fairly spanwise periodic regularity and to vary on a slow timescale [2]. This motivates the use of the steady *boundary layer approximations* for describing the evolution of both the linear calculation of optimal disturbances[16] and nonlinear calculation of streaks[10]. Similar to PSE, a parabolic approximation of the disturbance equations (2.2) is obtained, by scaling the mean flow and the disturbance as introduced in section 2.2 (the spanwise variables and coordinate are scaled as the wall-normal variables, i.e. with the boundary-layer thickness). We define the reference length L and the corresponding Reynolds number $\text{Re}_L = LU_\infty/\nu$. This is together with the boundary layer reference scale $\delta_L = (L\nu/U_\infty)^{1/2}$ used to scale the variables. Throughout this work, Reynolds number scaled with boundary layer scalings are denoted as Re , whereas the Reynolds number with PSE-scalings is R . They are related as $R = \sqrt{x\text{Re}}$.

The slow variation of streaks implies setting the streamwise fast-oscillating part of the disturbance (2.5) to zero, i.e. $\alpha = 0$, resulting in disturbance of the form,

$$\mathbf{q} = \hat{\mathbf{q}}(x, y)e^{i\beta t}. \quad (2.21)$$

Andersson *et al.*[16] used an optimization procedure and adopted an input-output point of view to calculate the initial conditions that generate the maximum growth of perturbation (2.21) in space. The output $\mathbf{q}_{out}(x, y)$ at $x > x_0$ is given with the input $\mathbf{q}_{in}(x_0, y_0)$ as initial condition. Because the initial value problem is linear and homogeneous, this can be written as

$$\mathbf{q}_{out} = \mathcal{A}\mathbf{q}_{in}, \quad (2.22)$$

where \mathcal{A} is a linear operator. By fixing the spanwise wave number β (scaled with δ_L) and the reference Reynolds number Re_L , they maximized the output disturbance energy at $x = x_1$ among all suitable input disturbances at $x = x_0$. The optimization problem is setup as an eigenvalue problem and solved iteratively by using the adjoint equations of the boundary layer approximation. The optimal disturbance is given by \mathbf{q}_{in} when optimization procedure has converged. The maximum spatial transient growth is defined as

$$G(x_0, x_1, \beta, \text{Re}_L) = \max_{\|\mathbf{q}_{in}=1\} \|\mathbf{q}_{out}\|^2, \quad (2.23)$$

where the norm $\|\cdot\|$ is any appropriate measure of disturbance, usually the energy (2.19) of the disturbance. Andersson *et al.*[16] chose $x_0 = 0.0$ and $x_1 = 1.0$ and showed that the optimal disturbance which experiences maximum growth ($G = 0.0022\text{Re}_L$) is a streamwise vortices with the spanwise wave number $\beta = 0.45$.

Furthermore, they found that the maximum growth (2.23) scales linearly with the distance from the leading edge, i.e

$$\overline{G}(x_0, x_1, \beta) = \frac{G(x_0, x_1, \beta, \text{Re}_L)}{\text{Re}_L} \quad \text{as } \text{Re}_L \rightarrow \infty. \quad (2.24)$$

As a consequence, the streamwise and spanwise directions are coupled. Consider the same dimensional problem but with two different scalings and $x_0 = 0$,

$$G(x_1, \beta, \text{Re}_L) = G(x_1^1, \beta^1, \text{Re}_L^1). \quad (2.25)$$

The variables are scaled as,

$$x^* = x_1 L = x_1^1 L_1, \quad \beta^* = \beta/\delta = \beta^1/\delta^1$$

where,

$$\begin{aligned} \delta_L &= U_\infty L/\nu, & \delta_L^1 &= U_\infty L_1/\nu, \\ \text{Re} &= U_\infty L/\nu, & \text{Re}^1 &= U_\infty L_1/\nu. \end{aligned} \quad (2.26)$$

Here, x^* and β^* are the dimensional streamwise location and spanwise number, respectively. By introducing $c^2 = L/L_1$, the right hand side of equation (2.25) is rewritten as,

$$G(x_1, \beta, \text{Re}_L) = G(c^2 x_1, \beta/c, c^2 \text{Re}_L). \quad (2.27)$$

Multiplying both sides by c^2/Re_L , letting Reynolds number go to infinity and using equation (2.24) the following relation is obtained,

$$c^2 \overline{G}(x_1, \beta) = \overline{G}(c^2 x_1, \beta/c). \quad (2.28)$$

As a consequence of equation (2.28) an optimal disturbance with a larger spanwise wave number will yield the same downstream development of a streak as an optimal disturbance with smaller spanwise wave number, but on a larger streamwise length scale, i.e the following relation is obtained,

$$x\beta^2 = \text{constant}. \quad (2.29)$$

To correctly account for the downstream development of streaks nonlinear calculations and the interactions of several disturbance modes are necessary. Thus, a convenient measurement of the streak amplitude is

$$A_s = \frac{1}{2} \left[\max_{y,z} \{u_s\} - \min_{y,z} \{u_s\} \right] \quad (2.30)$$

where u_s is the sum of the streamwise velocity component of all streak modes $(m, 0)$, i.e.

$$u_s = \sum_{m=0} u_m \cos(m\beta_0 z). \quad (2.31)$$

3 Numerical Procedure

3.1 Streaks with PSE Scalings

The results presented in this work are calculated using a non-local method to solve the nonlinear PSE, developed by Hanifi *et al.*[1] and called NOLOT. The compressible linear PSE is rewritten as a system of first order differential equations in order to use fourth-order compact difference scheme to approximate the derivative with respect to the wall-normal coordinate, rather than a less accurate finite difference scheme. The derivative with respect to the streamwise coordinate is approximated by a first and second order finite difference scheme. The nonlinear terms enter as a force on the right hand side of the equations.

The PSE scalings are appropriate for exponential growth. The assumption of slowly varying wall-normal mean flow is not valid for describing the downstream development of streaks, as contrast to boundary layer scalings (BLE). Levin and Henningson [15] presents the differences of the scalings in detail. The PSE is based on the scalings (2.6) and (2.7) applied to the linear disturbance equations (2.2) and the terms of $\mathcal{O}(1/R_0^2)$ and higher are neglected. The terms are presented in Table 3.1 and include the derivative of the wall-normal component of the mean flow uV_x and all elliptical terms except for p_x . The BLE scalings are based the basic assumption $\delta \ll L$ and the variables are scaled as described in section 2.2 and 2.3. All terms of $\mathcal{O}(1/R_0)$ and higher are neglected, which include the elliptical terms tabulated in Table 3.1.

The high order term in PSE scaling uV_x is only of order one in BLE scalings and the derivative of the pressure with respect to the streamwise coordinate, p_x is of the same order in both scaling but neglected only in the BLE. Furthermore, there exists one more issue worth addressing for readers that might use NOLOT to calculate streaks. The numerical formulation in NOLOT requires a system of first order ordinary equations, which results in a system eight equations with the following compressible variables $(u, v, T, w, \rho, u', v', T')$. In this formulation second derivatives in the wall-normal direction and wall-normal velocity amplitude function v have been eliminated by substituting the $\mathcal{O}(1/R_0)$ approximation of the continuity equation into the the wall-normal momentum equation. In this process the term u_{xy} is of $\mathcal{O}(1/R_0^2)$ and neglected in PSE approximation, but is only of $\mathcal{O}(1/\sqrt{R_0})$ in BLE scalings and must be included for all streak modes.

The solution procedure is different for exponential waves than for streaks. To correctly calculate the downstream development of the streaks using NOLOT and the PSE scalings, the higher order term uV_x (and u_{xy} in NOLOT) is added and the lower order term p_x is neglected. Thus in to order to calculate the interaction of the streaks and TS waves, it is necessary to solve two sets of equations. In Figure 3.1(a) we show downstream linear calculations of optimal disturbance with and without the higher order terms included in PSE.

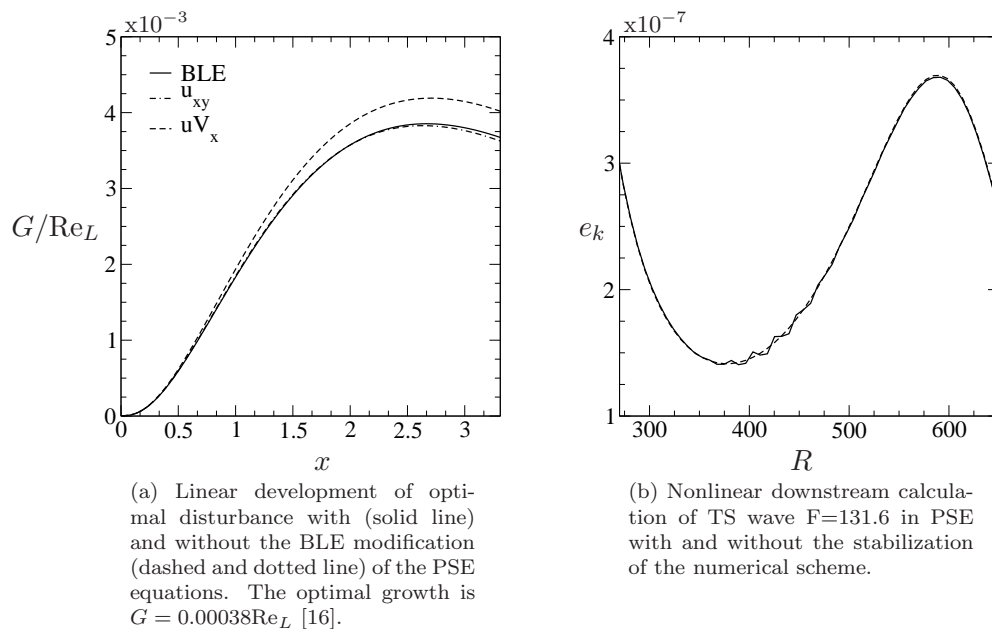


Figure 3.1: The numerical issues addressed in this work are the modification of the PSE equations to account for the algebraic growth and stabilization of nonlinear PSE numerical procedure.

Scalings	$\mathcal{O}(1)$	$\mathcal{O}(1/R_0)$	$\mathcal{O}(1/R_0^2)$
PSE		p_x	$u_{xx}, u\hat{V}_x, v_{xx}, w_{xx}$
BLE	$u\hat{V}_x$	$p_x, u_{xx}, v_{xx}, w_{xx}$	

Table 3.1: The neglected terms of the disturbance equations (2.2) for the two different scalings. The elliptical terms are of the form $u_{xx} = \hat{u}_{xx} + i\alpha\hat{u}$.

3.2 Removal of the Step-size Restriction for nonlinear PSE

The Parabolized Stability Equations are nearly parabolic in space. The remaining elliptical term \hat{p}_x , causes step-size restrictions for numerical schemes. If a too small step size is used, the numerical scheme becomes unstable and rapid oscillations is observed in the solutions (Figure 3.1(b)). The restriction[18] is found to be,

$$\Delta x = \frac{1}{|\alpha_r|}. \quad (3.1)$$

Andersson *et al.*[18] found a solution to this problem for linear PSE by approximating the streamwise derivative with a first-order implicit scheme and including a term proportional to the leading truncation error of the numerical scheme. The nonlinear PSE can be modified by the same method. This is necessary because the nonlinear interaction of the streaks and TS waves, requires accurate solutions to the PSE without the compromising the numerical stability of the scheme.

The PSE can be written as [19, 18]

$$\mathcal{L}\mathbf{q} = \mathbf{q}_x + \mathbf{F}. \quad (3.2)$$

The streamwise direction is discretized by a backward Euler method,

$$\mathbf{q}_{i+1} = \mathbf{q}_i + \Delta x(\mathcal{L}\mathbf{q}_{i+1} - \mathbf{F}_{i+1}), \quad (3.3)$$

with the truncation error,

$$\tau = \frac{\Delta x}{2} \mathbf{q}_{xx} + \mathcal{O}((\Delta x)^2/R_0^3). \quad (3.4)$$

The PSE contains only terms of $\mathcal{O}(1/R_0)$ and lower, therefore the higher terms of τ can be dropped. Using equation (3.2) the truncation error is rewritten as,

$$\tau = \frac{\Delta x}{2} \mathbf{q}_{xx} = \frac{\Delta x}{2} (\mathcal{L}_x \mathbf{q} + \mathcal{L} \mathbf{q}_x - \mathbf{F}_x). \quad (3.5)$$

By neglecting the term $\mathcal{L}_x \mathbf{q}$ for simplicity and adding a term $\mathcal{L} \mathbf{q}_x$ of same order as $\tau \in \mathcal{O}(1/R_0^2)$, Andersson *et al.*[18] introduced a new set of equations. In the same spirit, we drop the derivative of the forcing \mathbf{F}_x term for simplicity, and formulate a new set of equations as,

$$s \mathcal{L} \mathbf{q}_x + \mathcal{L} \mathbf{q} = \mathbf{q}_x + \mathbf{F}. \quad (3.6)$$

where s is a small positive number. The difference of equation (3.7) and (3.2) is of $\mathcal{O}(1/R_0^2)$, thus within the PSE approximation. In this way Andersson *et al.*[18] found a new critical step size for a stable numerical scheme as

$$\Delta x = \frac{1}{|\alpha_r|} - 2s \quad (3.7)$$

The number s has the function of a control parameter and is calculated at each time step in order to stabilize the PSE equations for small step sizes. In calculating the nonlinear interaction of streaks and TS wave this stabilization scheme is applied and verified. Nearly all forcing is accounted for by the streak, as its amplitude is between 0–25% of U_∞ , whereas the amplitude of the TS wave is very low $\sim 10^{-3}\%$ of U_∞ . For all the streak modes $(m, 0)$ and the mean flow distortion $(0, 0)$ the elliptic term p_x is zero and thus the stabilization is not necessary. The $3\mathcal{D}$ modes (n, m) excited by the forcing induced from the streak, have amplitudes of the same order as the $2\mathcal{D}$ TS wave $(0, n)$. These modes can be stabilized using the above scheme as long as their amplitudes are sufficiently low.

3.3 A Comparison to DNS

Brandt and Cossu [9] showed by numerical calculations that streaks with sufficiently high amplitudes are able to stabilize TS waves in zero pressure gradient boundary layers. The streaks used in [9] for stabilization were generated by the optimal disturbance shown in Figure 3.1(a) and first derived by Andersson *et al.*[16]. The optimal perturbation was used as inflow condition at the leading edge and its downstream development was followed until a streamwise location downstream, where different initial amplitudes were assigned to the streaks.

The numerical procedure in this work is similar to the work of Brandt and Cossu [9]. First, the optimal disturbance is calculated using an adjoint optimization technique based on a spectral collocation method involving Chebychev polynomials. Details about the scheme can be found in [15, 17]. Second, the optimal disturbance obtained is used as initial condition in NOLOT. The linear downstream development of the the optimal disturbance is calculated until a downstream station. At this location the nonlinear interaction of the streak and TS wave is initiated by the assignments of initial amplitudes.

Using the PSE, we calculate the nonlinear interaction of streaks and a TS wave and compare the results to the DNSsimulations of [9]. In the numerical experiments of Brandt and Cossu [9] five streaks with different amplitudes

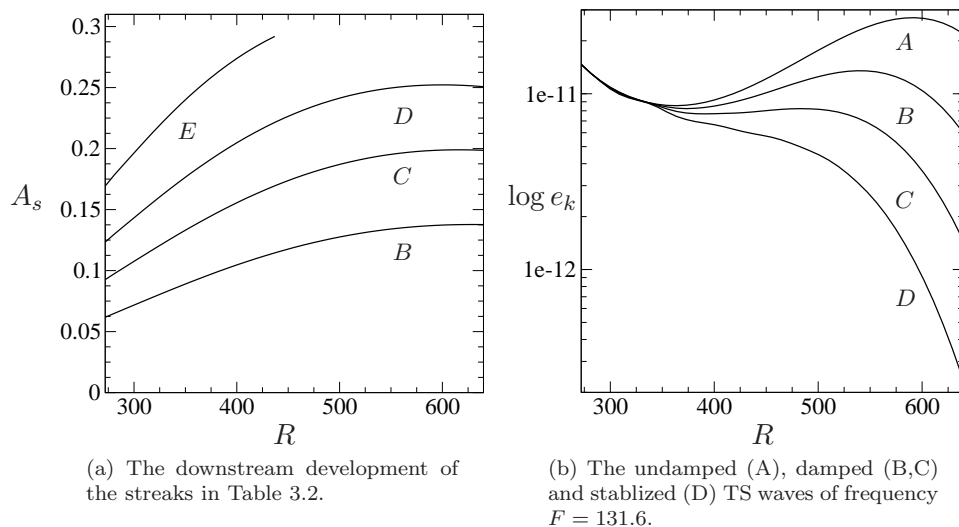


Figure 3.2: Stabilization of TS waves.

(2.30), labeled as B, C, D and E (Table 3.2 and Figure 3.2(a)) were initiated at $x = 0.4$. The reference Reynolds number was chosen as $\text{Re}_L = 185185$. This results in the initial location $R_0 = 272.1$ for nonlinear calculations and the local streak spanwise wave number (scaled with δ_0) $\beta = 0.282$. The frequency (2.18) of the TS waves is $F = 131.6$ (Figure 3.1(b)) and with an amplitude set sufficiently low in mode $(0, 1)$ to develop linearly downstream. Depending on the streak amplitude assigned in mode $(1, 0)$, 16–20 streak modes $(m, 0)$ and almost as many $3\mathcal{D}$ -modes $(m, 1)$ are excited by the forcing terms. The results of the nonlinear calculations are shown in Figure 3.2 and in Table 3.2.

The nonlinear downstream development of streaks are in good agreement with the DNS results of [9] (Table 3.2) The maximum streak amplitudes generated by PSE differ from the DNS results [9] with $\mathcal{O}(1/R_0^{3/2})$. The discrepancies are larger than the PSE approximation of $\mathcal{O}(1/R_0^2)$, but can also be attributed to the number of modes used in the nonlinear calculation and other numerical setups. In fact, in the nonlinear case, any initial discrepancy influence the downstream calculation.

The downstream development of the disturbance energy, defined as equation (2.19) are shown in Figure 3.2(b). The dampening effect on the TS wave is observed for all streaks and increases with the streak amplitude. For moderate

Streak	A_s^0	A_s^* PSE	A_s^* DNS	α_i^*
A	0.0000	0.0000	0.0000	0.0038
B	0.0618	0.1378	0.1400	0.0022
C	0.0927	0.1989	0.2018	0.0007
D	0.1235	0.2522	0.2558	-0.0013
E	0.1695	0.2914	0.3199	

Table 3.2: Initial and maximum amplitudes of the streaks used for stabilization. PSE results are produced in NOLOT and compared to DNS results of [9]. The maximum streak amplitude is denoted as A^* . The maximum growth rate α_i^* of the disturbance is defined in (2.20).

streak amplitudes a damping of the waves is observed which for streak D is sufficient to completely stabilize the TS wave. For the initial amplitude of $A_s^0 = 0.169$, streak E reaches a maximum amplitude of $A_s^* = 0.29$ when the PSE calculations diverge. In general, the accuracy of the PSE is reduced as the number of modes increase. For very high amplitudes such as streak E the calculations breakdown when the number of modes becomes very large. Note, that streak amplitude $A_s = 0.29$ is above the critical threshold beyond which secondary inflectional instability is observed [17, 9].

4 Results

4.1 The Mean Flow in the Presence of Streaks

Almost any cross-flow perturbation introduced into the boundary layer will develop into a streamwise streak through the so-called lift up effect. The streak then leads to a thickening and thinning of the otherwise uniform boundary layer [18, 2, 4, 14]. Consequently and in the same way as favorable pressure gradients, the influence of the streak on the stability of exponential disturbances manifests itself through the form of the modified velocity profile. We begin by characterizing the mean flow alteration in the presence of streaks with appropriate measures in order to relate the changes in the mean flow to the observed stabilization effect.

The mean distortion flow u_0 and the velocity profile of the boundary layer flow $\tilde{U} = U + u_0$ in the presence of the streaks A, B, C and D in Table 3.2 are illustrated in Figure 4.1(a) and 4.1(b). The mean flow distortion modifies the velocity profile into a “fuller” shape close to the wall, and it forces the velocity to decrease in the outer part of boundary layer. This decrease can lead to an inflection point in the velocity profile [18, 4]. In order to estimate the possibility for inviscid instability, the profiles of the second derivative of the mean flow in the presence of the streaks are plotted in Figure 4.1(c). The second derivative in the outer region is different from zero with a wide margin, but increase with the streak amplitude and may result in inflectional instability [14, 4] for higher streak amplitudes. The increase of the mean velocity close to the boundary layer is on the other hand, responsible for the stabilizing effect of streaks on TS waves. Clearly, the effects of the streak on the mean velocity are increased with the streak amplitude.

We define the excess and deficit of the mean flow as the maximum and the minimum value of the mean flow distortion in the streamwise direction, i.e.,

$$u^+ = \max_y \{u_0\}, \quad u^- = \min_y \{u_0\}. \quad (4.1)$$

In Figure 4.2, the velocity excess u^+ and deficit u^- are shown for streaks B, C and D as a function of the streamwise coordinate. The velocity excess increases with the streak amplitude and based on the earlier discussion, it can be predicted that the most beneficial stabilization effect of a streak should be observed at the location, where the velocity excess is maximum. This location is about $R \sim 700$ and slightly shifted upstream for increasing streak amplitudes. Figure 4.2 also shows, that downstream the velocity excess rapidly decreases towards zero. The velocity deficit attains a minimum further downstream at a location $R \sim 800$ and is shifted downstream for larger amplitudes. Furthermore, the deficit approaches a constant limit downstreams.

In order to investigate the manner which the mean flow excess and deficit affect the stability of viscous exponential disturbances, we define the total sum of the mean flow excess and deficit along the plate. This is a convenient measurement of the overall change of the velocity profile and will be useful in

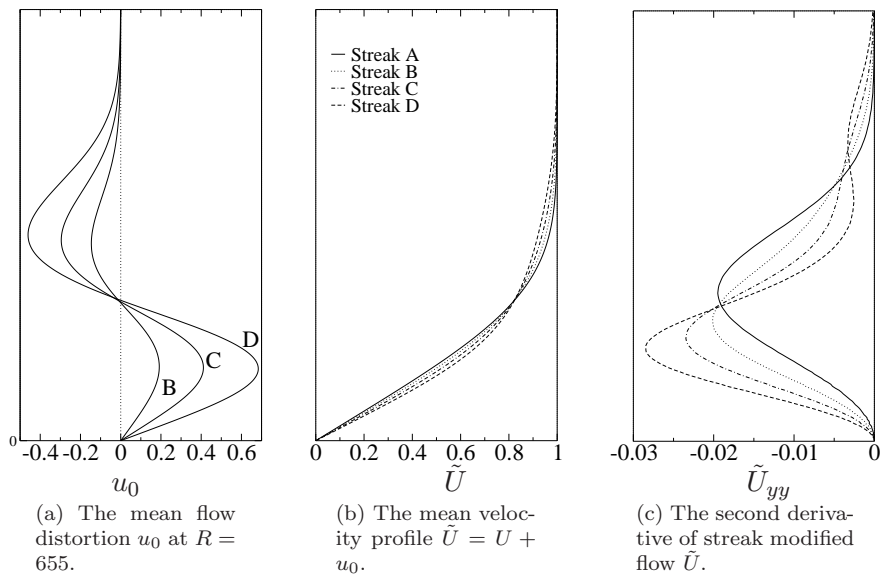
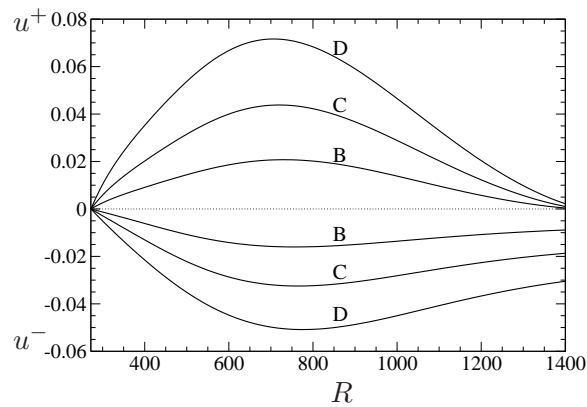


Figure 4.1: The mean flow modifications due to streaks A, B, C and D.

Figure 4.2: The downstream development of mean flow excess u^+ and deficit u^- in the presence of streak B, C and D.

the studies of the streak in the coming sections. Thus, we define,

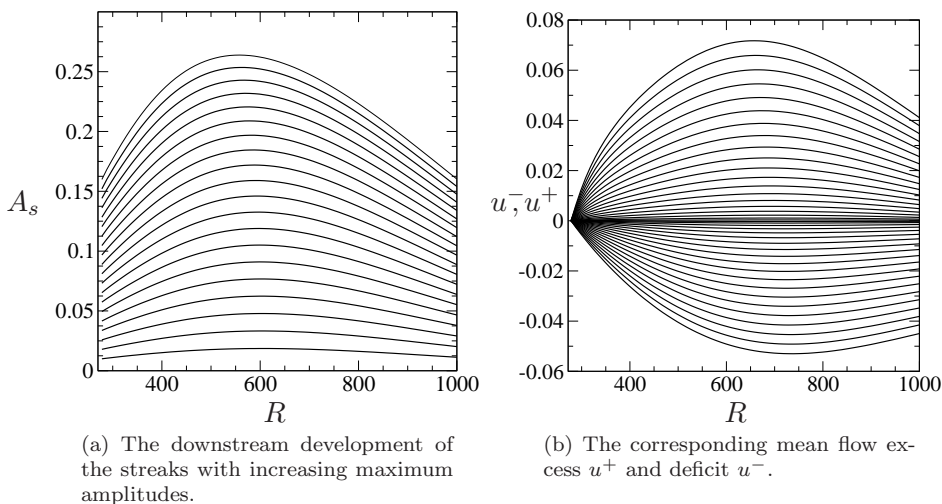
$$U^+ = \int_{x_0}^{x_1} u^+ dx, \quad U^- = \int_{x_0}^{x_1} u^- dx \quad (4.2)$$

where x_0 and x_1 define the streamwise region of interest. Furthermore, the difference of the total mean flow excess and deficit is denoted as

$$\Delta U = U^+ - U^-. \quad (4.3)$$

4.2 Characteristics of the Streaks Investigated

In this section we define three sets of streaks and investigate how they alter the mean flow. The first case is a family of streaks whose amplitudes are varied and will be from here denoted case A. These streaks are developed from an

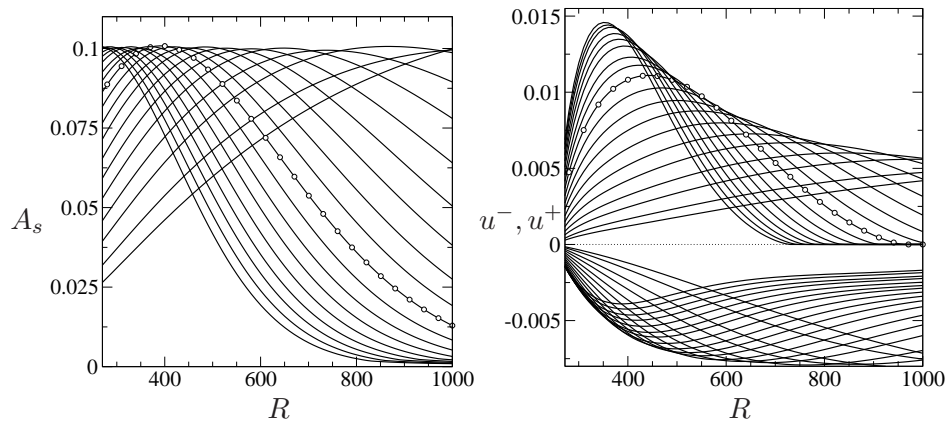
Figure 4.3: The streaks and mean flow distortions composing set A .

optimal disturbance that is generated close to the leading edge and optimized for the downstream location $x_1 = 1$ and spanwise wave number $\beta = 0.45$. The reference Reynolds number (defined in section 2.3) is $\text{Re}_L = 193210$. The linear downstream development of the streak is calculated until the streamwise position $x = 0.4$. At this location the nonlinear calculations are initiated by assigning a series of initial amplitudes A_0 to the streak. The streaks in this set attain maximum amplitudes A_s^* between 0.0–0.25 with a step-size of $\Delta A_s^* \sim 0.012$. The nonlinear downstream development of the streaks in case A is shown in Figure 4.3(a) with their corresponding mean flow distortions in Figure 4.3(b). For this particular choice of parameters the streaks have a fairly constant amplitude for a large downstream distance. The upstream shift of the location of the maximum streak amplitude observed in Figure 4.3(a), was also noted in the simulations of Brandt and Cossu[9]. The same upstream shift is observed for the corresponding amplitudes of mean flow excess in Figure 4.3(b), whereas the maximum mean flow deficit propagates downstream. This implicates that the difference of the flow excess and deficit, $u^+ - u^-$ at all streamwise locations grows with the streak amplitude.

The importance of the spanwise wave number of the streak is studied with two series of perturbations that are similar to each other. These streaks are generated from a set of optimal disturbances with spanwise wave numbers β (scaled with Re_L) between 0.0–1.0 and the step-size $\Delta\beta \sim 0.05$. The streamwise region, x_0 – x_1 is the same as for the optimal disturbance used as initial condition in case A , but the reference Reynolds number is $\text{Re}_L = 156250$. For each optimal disturbance an initial amplitude at $x = 0.4$ is carefully chosen

Set	β	A_s^*	R_0	R_1
A	0.45	0–0.25	278	1000
B1	0.0–1.0	0.1	250	1000
B2	0.0–1.0	0.2	250	1000

Table 4.1: The three sets of streaks A , B_1 and B_2 used in the parametric studies. Here Reynolds number is defined as $R = U_\infty \delta / \nu$ and β is scaled with $\text{Re}_L = U_\infty L / \nu$.



(a) Different initial amplitudes are chosen in order to obtain the fix downstream amplitude $A_s^* = 0.1$. Larger spanwise wave numbers result in more upstream maximum amplitudes.

(b) The mean flow excess and deficit of the streaks.

Figure 4.4: The streaks composing set B have the same maximum amplitudes and shapes. The streak and mean flow distortion marked with circles attain the maximum total velocity excess U^+ .

so that the maximum amplitudes of all downstream streaks in the set attain a fix value. For the first set of “ β -streaks”, denoted as B_1 , the fixed maximum amplitude is $A_s^* = 0.1$ and for the second set B_2 , the maximum amplitude is $A_s^* = 0.2$. The evolution of streaks in case B_1 in the streamwise coordinate is illustrated in Figure 4.4(a) with their corresponding mean flow distortion in Figure 4.4(b). The fix maximum streak amplitude moves upstream with increasing spanwise wave numbers. Due to the scaling properties (2.29) of the boundary layer approximation, the mean flow excess and deficit grow on a smaller streamwise scale for increasing wave numbers, which also result in the observed upstream shift of the flow excess. The downstream development and characteristics of streaks in case B_2 are identical to case B_1 , except that the amplitudes are larger. The purpose of set B_1 and B_2 is to partly investigate the optimal choice of a streamwise location of the streak amplitude in order to stabilize a TS wave and partly to investigate the effect of spanwise wave number on the TS energy. The characteristics of the three cases A , B_1 and B_2 are presented in Table 4.1.

Total mean flow excess and deficit

For now, we assume that the mean flow which attains the largest total flow excess U^+ in the unstable region of viscous disturbances, is optimal for stabilizing the flow. This prediction will be put to the test in the following sections as we aim at obtaining the most favorable mean flow by the choice of a more optimal streak. The dependences of the mean flow characteristics (4.2),(4.3) on the streak amplitude in case A and spanwise wave number in case B_1 and B_2 are shown in Figure 4.5. The total flow excess U^+ , deficit U^- and the difference ΔU is plotted against the maximum streak amplitude of streaks in case A in Figure 4.5(a). The summation of u^+ and u^- is carried out from the initial streamwise location $R_0 = 278$ until the $R_1 = 1000$. The total mean velocity excess U^+ grows almost exponentially with the streak amplitude and U^- decays at a somewhat slower rate. Furthermore, it is found that ΔU grow

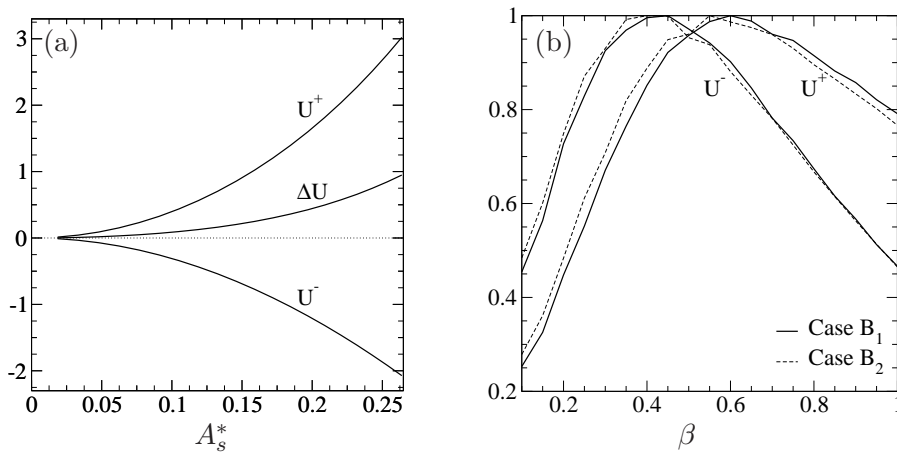


Figure 4.5: The total flow excess U^+ , deficit U^- and their difference ΔU for all three sets A , B_1 and B_2 versus the maximum streak amplitude A_s^* and spanwise wave number β .

with A_s^* , implicating that for increasing streak amplitudes the total velocity excess between R_0 and R_1 becomes greater than the total deficit.

Figure 4.5(b) shows the total excess and deficit for the streaks in case B_1 and B_2 , where U^+ and U^- have been normalized with the maximum and minimum spanwise value respectively. The maximum value of U^+ in the set B_1 is obtained for a streak with the spanwise wave number $\beta^* = 0.6$ and with the location of its maximum amplitude at $R^* = 400$. The corresponding streak in set B_2 is obtained for $\beta^* = 0.55$ which also results in streamwise location $R^* = 400$ of the maximum amplitude. In an analogous way, the streaks with maximum total mean flow deficits in B_1 and B_2 are shifted by $\Delta\beta = 0.05$, but have the same streamwise location of the maximum amplitudes $A^* = 0.1$ and $A^* = 0.2$. This can be explained from the previously observed upstream shift of the profiles with higher amplitudes (shown in Figure 4.2). Technically, it is possible to cancel the upstream shift of the streak profile due to the increase of amplitude by decreasing the spanwise wave number. Therefore, it is possible to assume at this point, that the most beneficial stabilization effect between $R_0 = 250$ and $R_1 = 1000$ is obtained by the streak whose maximum amplitude is located at $R^* = 400$. Hence, to locate the streamwise position of the maximum streak amplitude for an optimal stabilization it is enough to consider only one set. The results presented in the following sections are mainly focused on streaks in B_1 . In order to measure the actual stabilization effect, it is necessary to calculate the stability of TS waves in the presence of streaks. This matter is investigated in the next section.

The streak shape

Note that the streaks in this investigation have the same basic shape, but on different streamwise scales. This is a consequence of the coupling of the spanwise and streamwise scales (2.29) explained in section 2.3. For a different choice of parameters optimal disturbances with greater downstream growth can be obtained. However, they do not necessarily develop into a streak with the most efficient stabilization effect. Levin and Henningson [15] showed that optimal disturbances with greater growth can be created by choosing an initial streamwise location further downstream. This will result in a streak with a shape

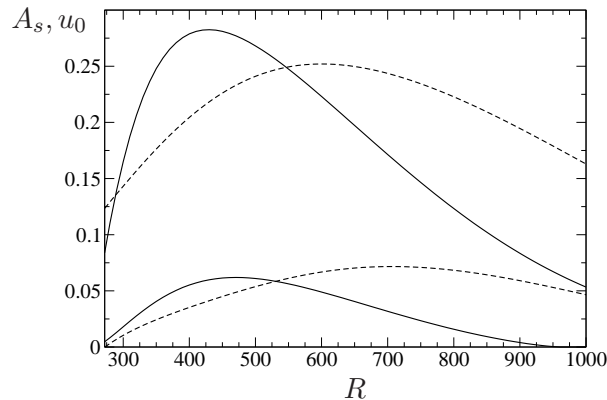


Figure 4.6: Streak of different shapes. The streak and mean flow distortion used in this work (dashed) keep a fairly high amplitude downstream, whereas the streak and mean flow distortion with greater growth (solid) rapidly decay downstream.

characterized by strong gradients. In Figure 4.6 we compare the streak used in this investigation with the streak calculated from the optimal disturbance of [15]. The mean flow distortion of the streak from Levin & Henningson ?? rapidly decreases after it reaches its maximum value, whereas the streak used in this work keeps the mean flow fuller for a large streamwise region.

4.3 The Stabilizing Effect of the Streak Amplitude

In order to measure the stabilizing effect of streaks, we calculate the nonlinear downstream evolution of Tollmien-Schlichting waves in the presence of streaks in set A , B_1 and B_2 . The TS wave growth in the streamwise direction is measured with the N-factor (2.20), maximum growth rate α_i^* (2.20) and the disturbance energy e_k (2.19) integrated in the streamwise direction, i.e

$$E = \int_{x_0}^{x_1} \int_0^{y_{max}} (\hat{u}^2 + \hat{v}^2 + \hat{w}^2) dx. \quad (4.4)$$

The streamwise location x_0 and x_1 correspond to the locations of Branch I and II on the neutral stability curve in Figure 2.2 of the undamped TS wave. For damped disturbances, the streamwise location of Branch I on the neutral stability curve moves downstream and Branch II moves upstream. This is clear from the downstream development of disturbances in Figure 3.2. The energy ratio for the N-factor (2.20) is calculated using the “moving” locations of Branch I and Branch II of the damped TS wave.

Three TS waves with the frequencies (2.18) $F_1 = 90$, $F_2 = 131$ and $F_3 = 170$ and of sufficiently low amplitudes to ensure a linear downstream evolution are used in this work. The results of the calculation of the boundary layer stability in the presence of streaks in set A is presented in Figure 4.7. The maximum growth rates α_i^* are plotted against the maximum streak amplitudes A^* in Figure 4.7(a). The growth rate for all three frequencies decrease with the amplitude as previously observed [9, 11, 12]. For negative growth rates the TS waves are completely stabilized. The more upstream TS wave with $F_3 = 170$ is totally stabilized at an amplitude of $A^* = 0.220$, whereas the amplitudes required for $F_2 = 131$ and $F_1 = 90$ are $A^* = 0.209$ and $A^* = 0.195$, respectively. The streamwise location of the maximum amplitude of the streaks is attained between $R \sim 550-700$. Thus the stabilizing effect experienced by the three disturbances is different because the streak amplitude between Branch I and

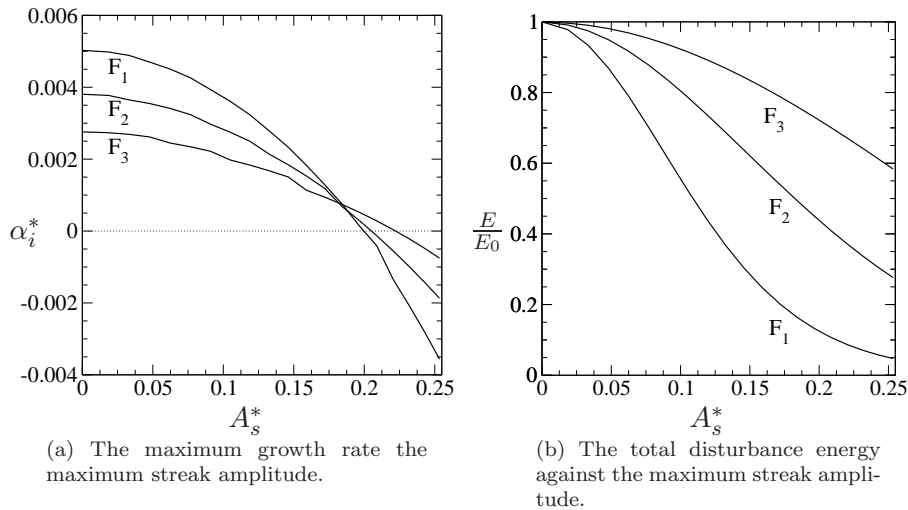


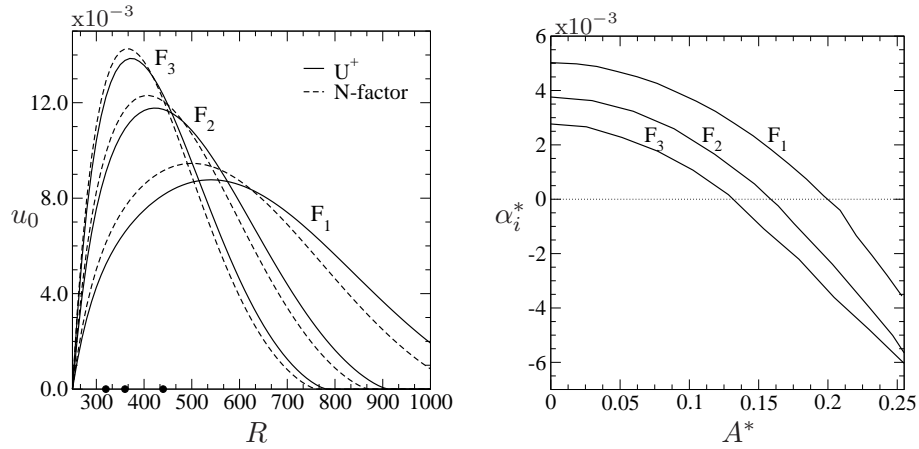
Figure 4.7: The effect of streaks in set A on the energy and growth rate of TS waves with the frequencies are $F_1 = 90$, $F_2 = 131$ and $F_3 = 170$.

II is different for each disturbance. For $F_1 = 90$, which is the TS wave with the greatest downstream growth, the total suppression of the disturbance is observed just below 20% of U_∞ as the maximum streak amplitude is attained near the location Branch II. In contrast, the streak amplitude has not yet reached half of its maximum amplitude in the unstable streamwise region for $F_3 = 170$.

Clearly, the decline of the disturbance growth rate increase with the streak amplitude. Generally, for streak amplitudes over 20% of U_∞ the stabilization effect is noticeably intensified. This can be compared to the increase of total velocity excess U^+ shown in Figure 4.5(a) of streaks in A . The nearly exponential rate of U^+ with the A_s^* between R_0 and R_1 is likely to be the reason for the strong increase of the stabilization effect for higher amplitudes. For a transition delay protocol, it is of interest to investigate what range of frequencies that can be stabilized in the presence of one streak. Using the streak with the highest amplitude $A_s^* = 0.25$ in set A , we were able to completely stabilize waves up to the frequency $F = 70$, with the streamwise location of branch II at $Re \sim 950$. The total disturbance energy in the presence of streaks in set A , normalized with the corresponding energy of the undamped disturbance is shown in Figure 4.7(b). The TS wave of frequency F_3 experiences the most energy loss and F_1 the least.

4.4 The Stabilizing Effect of the Spanwise Wave Number of the Streak

The stabilizing effect of a streak is fundamentally connected to its amplitude. However, due to the downstream growth and decay of the streak, the search of an optimal stabilizing streak depends on which TS wave that is to be stabilized. In this section, we calculate the stability of the Blasius boundary layer to TS waves in the presence of streaks in set B_1 and B_2 . Using these streaks with varying spanwise wave numbers and fix maximum amplitudes we can locate the streamwise position where the most stabilizing effect, i.e. greatest streak



(a) The mean distortion flow of the streak with largest total velocity excess U^+ (solid lines) between Branch I and II compared the mean distortion flow of the streak obtained from calculating the N-factor (dashed lines) of the disturbances.

(b) The growth rates of the three disturbances in the presence of the optimal stabilizing streaks in (a) against the maximum streak amplitude.

Figure 4.8: Using the optimal stabilization streak obtained from calculating the N-factor in (a), the growth rates of the frequencies $F_1 = 90$, $F_2 = 131$ and $F_3 = 170$ are calculated. The streamwise locations of Branch I are marked with filled dots in (a), with F_3 farthest left and F_1 farthest right.

amplitude, should be applied in order to damp a TS wave optimally.

N-factor of Disturbances

The N-factors for F_1 , F_2 and F_3 in the presence of streaks in case B_1 are plotted in Figure 4.10. The decrease of the N-factors show that the dampening effect is observed in the presence of all streaks in B_1 . However, for streaks with small spanwise wave numbers that attain high amplitudes downstream, only a slight decrease of the N-factor is observed. This is also the case for the “upstream streaks” with large values of β . Clearly, for each frequency there exists an optimal streak with a spanwise wave number denoted as β_N^* , that gives the most stabilizing effect. This streak attains its maximum amplitude at streamwise location, denoted as Re_N^* , close to Branch I of the undamped TS wave. The streamwise locations of Branch I and Re_N^* are listed in table 4.2.

Figure 4.10 shows the total velocity excess U^+ , the deficit U^- and the difference ΔU against the spanwise wave number β of the streaks in B_1 . The local mean profile excess u^+ and deficit u^- are summed between the streamwise locations of Branch I and Branch II of each frequency in order to obtain U^+ and U^- . In table 4.2 the spanwise wave number (denoted as β_U^*) of the streak that results in the largest mean velocity excess for each TS wave is compared to the optimal wave number obtained by calculating the N-factor β_N^* . Taking into consideration that the step-size of the spanwise wave numbers of the streaks in the set B_1 is $\Delta\beta = 0.05$ the optimal values of β_N^* and β_U^* differ only one step-size for all frequencies.

In Figure 4.8 the mean flow distortions corresponding the optimal stabilizing streaks that was obtained by calculating the N-factor of the TS waves are compared to the mean distortion flows that are estimated to have the greatest

effect due to the largest streamwise mean flow excess. By the nearly complete collapse of the profiles, we conclude that the total mean flow excess is an appropriate measurement and method of prediction of the stabilizing effect of streaks. Our previous assumption, i.e. the mean flow which attains the largest total flow excess in the unstable region of viscous disturbances is optimal for stabilizing the flow, is justified. We can also conclude that the decrease of the mean flow in outer part of the boundary layer and the difference ΔU does not influence the stabilizing effect of the mean flow noticeably. In Figure 4.8(b) the maximum growth rates of F_1 , F_2 and F_3 in the presence of streaks that attain its maximum amplitude close to branch I of the disturbances are plotted. The maximum amplitude required in order to completely stabilize the $F_3 = 170$ is about $A_s^* \sim 0.13$ and for $F_2 = 131$ it is $A_s^* \sim 0.16$. Comparing Figure 4.8(b) with Figure 4.7(a) it is clear that maximum amplitude required to stabilize the disturbances is considerably decreased.

Energy of Disturbances

In Figure 4.9, the total disturbance energies E for F_1 , F_2 and F_3 are plotted against the spanwise wave number β of streaks in case B_1 . The energies of dampened disturbances are normalized with the energy of the corresponding undampened disturbance. For all three frequencies, disturbance energy decays until streaks of very large spanwise wave numbers become present. Note that the total disturbance energy (4.4) does not reveal the stability of the disturbance. It is possible and often the case that the total disturbance energy is decreased considerably in the presence of a streak, but the disturbance still experiences spatial growth downstream. The streaks with spanwise wave numbers (called β_E^*) that minimize the disturbance energies for F_1 , F_2 and F_3 attain their maximum amplitudes far upstream of the locations of Branch I. Consequently, these streaks do not dampen the TS waves noticeably compared to more downstream streaks. The streamwise locations of the maximum streak amplitudes that are associated with β_N^* , β_U^* and β_E^* are reported in Table 4.2.

Hence, we can expect that the spanwise dependence of the streak-modified mean flow to be of particular importance for the disturbance energy. In a linear analysis of Brandt and Cossu [11] it was showed that the stabilizing effect of streaks could be attributed to the spanwise shear \tilde{U}_z of the streak-modified mean flow $\tilde{U} = U + u_0$. The problem was formulated as an extension of the Orr-Sommerfeld equations, where the streamwise component of mean flow is spanwise dependent, i.e. $(U(y, z), 0, 0)$. The expression for disturbance energy in the presence of streaks was derived and shown to consist of energy production and dissipation terms. By numerical experiments it was found that the energy production is decreased with the streak amplitude, but the importance of the spanwise wave number for the disturbance energy was left somewhat unclear. The energy production term arising from the spanwise dependence of the mean flow is however, associated with the spanwise shear \tilde{U}_z , which is increased for larger spanwise wave numbers. Thus, the prediction[11] of the decrease of disturbance energy with increasing β can be confirmed with our results in Figure 4.9.

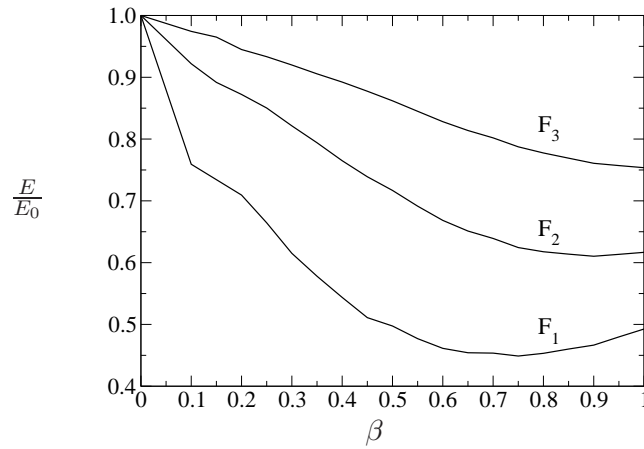


Figure 4.9: The total disturbance energies for F_1 , F_2 and F_3 in the presence the streaks in B_1 . $E/E_0 = 1.0$ is the energy for the undamped disturbances.

F	β_N^*	β_U^*	β_E^*	Branch I	Branch II	Re_N^*	Re_U^*	Re_E^*
90	0.45	0.5	0.75	440	790	480	450	330
131	0.65	0.7	0.9	360	590	370	350	290
170	0.85	0.9	1.0	320	480	300	290	260

Table 4.2: The spanwise wave numbers obtained from the N-factors of disturbances are denoted as β_N^* and compared to the total velocity excess β_U^* of the mean flow. The respective streamwise locations Re_N^* and Re_U^* of the location of the maximum streak amplitude corresponding to β_U^* and β_N^* are given together with the location of Branch I for each disturbance. The analogous values are given for the disturbance energy, denoted as β_E^* and Re_E^* .

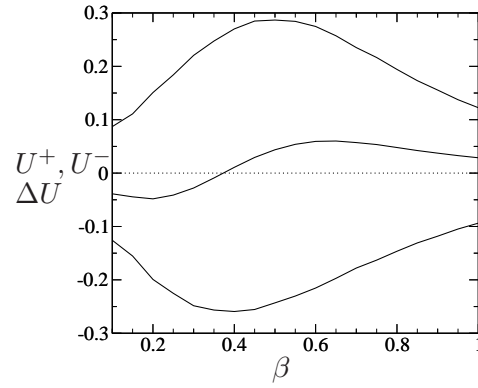
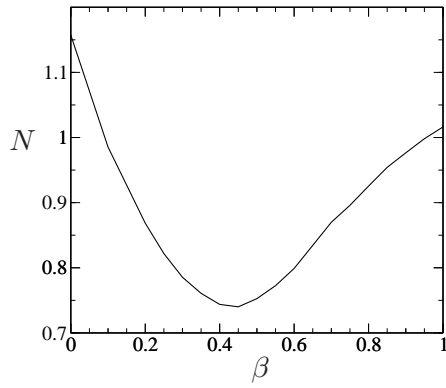
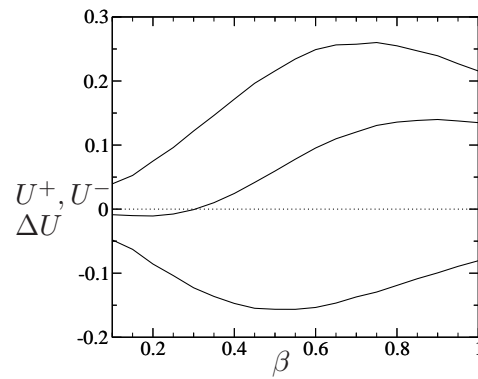
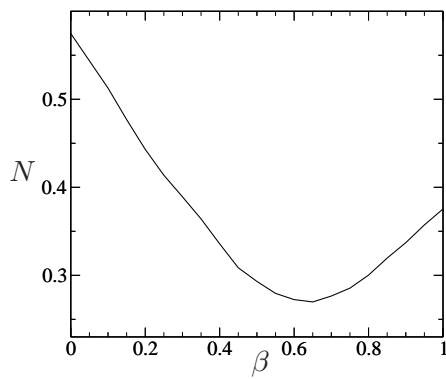
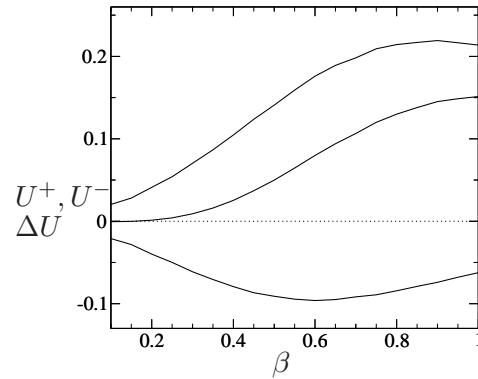
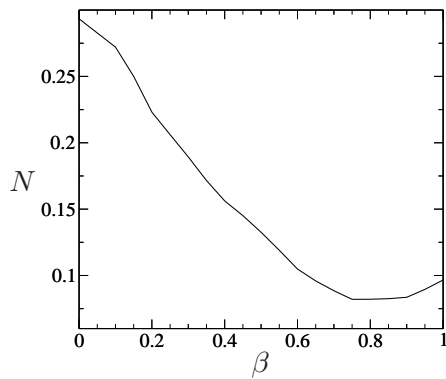
$F_1 = 90:$  $F_2 = 131:$  $F_3 = 170:$ 

Figure 4.10: The left column of figures present the N-factor for the TS waves F_1 , F_2 and F_3 against the spanwise wave number β . The right column of figures illustrate the total mean flow characteristics U^+ (top curves), U^- (bottom curves) and ΔU calculated for the unstable region of TS waves F_1 , F_2 and F_3 .

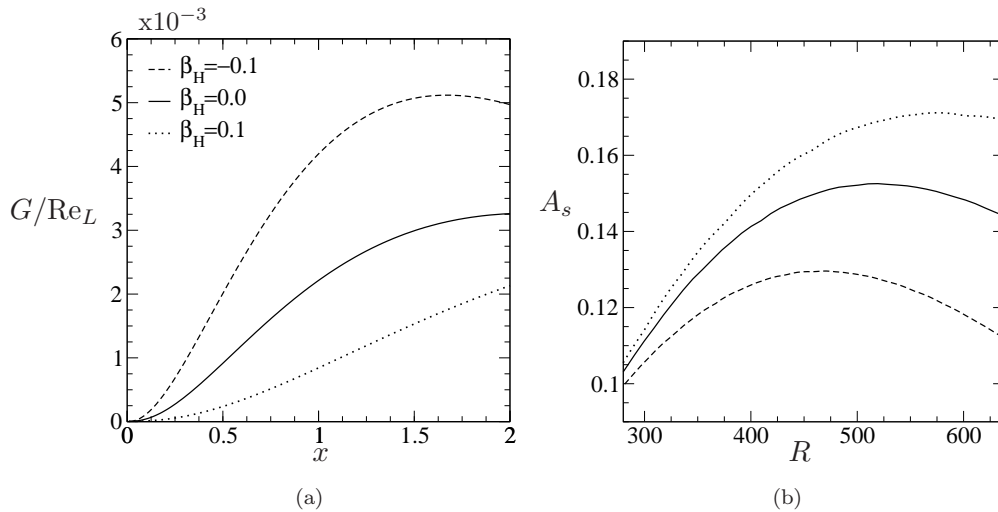


Figure 4.11: The linear downstream development of optimal disturbance and nonlinear development of streaks.

4.5 The Effect of Pressure Gradients on Streaks

We continue to investigate the mean flow on which streaks and TS waves interact, for a favorable and an adverse pressure gradient. In section 2.2 we introduced flat-plate boundary layer effects due to pressure gradients. In Figure 4.11(a) the linear downstream development of three optimal disturbances in three boundary layers with $\beta_H = -0.1$, $\beta_H = 0$ and $\beta_H = 0.1$ is shown. The optimal disturbance is calculated from the leading edge and optimized for the streamwise location $x_1 = 1$ and $\beta = 0.45$. Clearly and as Levin and Henningson [15] showed the algebraic growth increase for a negative pressure gradient. In Figure 4.11(b) however, we observe that the nonlinear downstream growth of streaks in the three boundary layers have the reverse order of growth. The growth in this case seem to be larger for positive pressure gradients. As in the previous calculations in this work, we use the optimal disturbance as initial condition at a downstream initial position $x = 0.4$. In this procedure, the optimal disturbances with larger growth rates at $x = 0.4$ develop into streaks with greater downstream growth. This effect is also observed when streaks generated from optimal disturbances of varying spanwise wave numbers are followed in the streamwise direction. Optimal disturbances with small spanwise wave numbers grow faster, but develop into streaks with less downstream growth compared to streaks originating from optimal disturbances with larger spanwise wave number.

In Figure 4.12 we show the downstream development of a TS wave of frequency $F = 131$ in the absence and presence of streaks in boundary layers with favorable and adverse pressure gradients. The stabilization effect of streaks on TS waves is also observed in these boundary layers, and as one may expect from the streak shapes in Figure 4.11(b) the dampening effect of the TS wave increase for streaks in favorable pressure gradient and decrease for adverse pressure gradients. Note that, favorable pressure gradient also modify the velocity profile of flat-plate boundary layers into a fuller shape close the wall, similarly to the spanwise modulation of the mean flow caused by streaks.

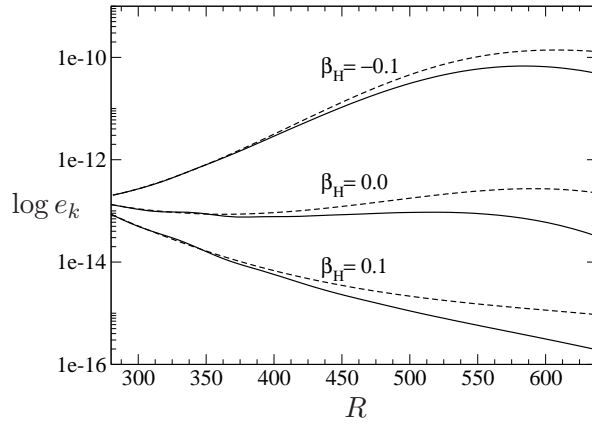


Figure 4.12: The downstream development of a TS wave of frequency $F = 131$ in the absence (dashed lines) and presence (solid lines) of the streaks in Figure 4.11(b).

4.6 Conclusions

In this study, we have performed parametric studies of the amplitude and spanwise wave number of streaks and characterized the induced mean flow distortions. We have also investigated the stability of the mean flow in the presence of the streaks. The main results can be summarized as follows.

1. The maximum growth rates and energies of TS waves with three different frequencies has been calculated in the presence of a set of streaks with maximum amplitudes between 0–25% of U_∞ . It was found that the stabilizing effect of the streak is considerably increased for higher amplitudes. This can be attributed to the nearly exponential rate of increase of the mean flow excess with the streak amplitude in the presence of the same set of streaks.
2. The N-factors and energies of the TS waves was calculated in the presence of a set of streaks with varying spanwise wave numbers and fixed maximum streak amplitudes. In the calculations of the N-factors, it was found that the optimal stabilization effect is obtained for streaks with a location of the maximum amplitudes close to Branch I of the TS wave. The same or a “neighboring” streak in the set attains the largest total mean flow excess in the unstable streamwise region of the disturbances. The mean velocity deficit in the outer parts of the boundary layer does not influence the stability characteristics of the mean flow for TS waves noticeably. The minimum disturbance energy is obtained in the presence of streaks with large spanwise wave numbers and whose maximum amplitudes are far upstream of the location of the Branch I of the disturbances.

5 Discussion

The PSE equations has been modified to account for the algebraic growth of streaks. The nonlinear downstream development of streaks with a maximum amplitude below the critical amplitude threshold for inflectional instability, can be calculated using these equations. The nonlinear interaction of TS waves and steady streamwise streaks, and the stabilizing role of the streaks on the mean flow has been verified with previous DNS results [9].

The dampening of the growth for TS waves in the presence of streaks has been attributed to the mean flow excess close to the boundary layer wall by previous authors [9, 14]. We found that the optimal stabilization effect obtained by calculating the growth rates of TS waves is observed when the total mean flow excess is close to its greatest value in the unstable streamwise region of a disturbance. Using this as a measure of the stabilization, it is possible to find the optimal stabilizing streak without actually calculating the stability of the flow to TS waves. Furthermore, as the mean flow excess increase at nearly exponential rate with streak amplitude, one should foremost aim at generating a streak with a high amplitude which is preserved for large streamwise distance.

In a transition delay protocol, one may stabilize the mean flow not only with a streak that maintains high amplitude throughout the unstable region of exponential disturbances, but also a streak that is positioned optimally. This may prove to be important if the streak amplitude is insufficient for stabilizing disturbance present very upstream or downstream in the boundary layer. Our results show that, in order to achieve flow stability effectively the optimal location of maximum streak amplitude is not close to Branch II of the disturbance. It is found that the greatest total velocity excess is obtained for streaks, whose location of the maximum amplitude is close to Branch I of the disturbances. This observation can be specific to the particular streak profile considered in this investigation. However, studies of other stabilizing methods which act on the mean flow has shown that TS waves are the most “sensitive” close to Branch I. For example, Pralits *et al.*[8] showed by a sensitivity analysis involving PSE adjoint equations that the optimal distribution of steady suction in order to damp the TS wave is close to Branch I.

Optimal stabilizing streaks are not necessarily obtained by using optimal disturbances with large downstream growth[15] as initial conditions. In general, these optimal disturbances are associated with very high growth rates and therefore result in a very steep growth and decay of the streak amplitude. Furthermore, the laminar streaks that are induced by free-stream turbulence are remarkably similar to those optimal growing streaks calculated by Andersson *et al.*[16] and that have been used in this work to stabilize the boundary layer. However, streamwise streaks can be expected to arise whenever the boundary layer is subject to weak perturbations in the spanwise direction. Hence, there exists different methods of streak generation, making it possible to introduce streaks of varying shapes and amplitudes into the boundary-layer. Further investigation of the streak amplitude threshold for different streak profiles (than used here and [9, 17]) is necessary in order to possibly obtain streaks of higher

amplitudes without the occurrence of inflection points in the velocity profile.

Acknowledgements

I thank my supervisor Ardeshir Hanifi at FOI for proposing this stimulating and challenging task and unconditionally taking time to answer the endless number of questions. I also appreciate the advice from Luca Brandt and Martin Byström from KTH Mechanics.

A PSE Matrices

For incompressible flow the matrices for the PSE are,

$$\begin{aligned}
 A &= \begin{pmatrix} \Delta_{mn} + U_x & U_y & 0 & i\alpha_{mn} \\ 0 & \Delta_{mn} + V_y & 0 & 0 \\ 0 & 0 & \Delta_{mn} & im\beta \\ i\alpha_{mn} & 0 & im\beta_0 & 0 \end{pmatrix}, \\
 B &= \begin{pmatrix} V & 0 & 0 & 0 \\ 0 & V & 0 & 1 \\ 0 & 0 & V & 0 \\ 0 & 1 & 0 & 0 \end{pmatrix}, \\
 C &= \begin{pmatrix} -\frac{1}{Re} & 0 & 0 & 0 \\ 0 & -\frac{1}{Re} & 0 & 0 \\ 0 & 0 & -\frac{1}{Re} & 0 \\ 0 & 0 & 0 & 0 \end{pmatrix}, \\
 D &= \begin{pmatrix} U & 0 & 0 & 1 \\ 0 & U & 0 & 0 \\ 0 & 0 & U & 0 \\ 1 & 0 & 0 & 0 \end{pmatrix}
 \end{aligned} \tag{A.1}$$

where

$$\Delta_{mn} = -in\omega + i\alpha_{mn}U + \frac{\alpha_{mn}^2 + m^2\beta^2}{Re}.$$

The forcing is,

$$f_{mn} = \sum_k \sum_l \begin{pmatrix} i\alpha\hat{u} + \hat{u}_x & \hat{u}_y & im\beta\hat{u} \\ i\alpha\hat{v} + \hat{v}_x & \hat{v}_y & im\beta\hat{v} \\ i\alpha\hat{w} + \hat{w}_x & \hat{w}_y & imn\beta\hat{w} \\ 0 & 0 & 0 \end{pmatrix}_{k,l} \begin{pmatrix} \hat{u} \\ \hat{v} \\ \hat{w} \\ 0 \end{pmatrix}_{m-k,n-l}. \tag{A.2}$$

Bibliography

- [1] A. Hanifi, S. Hein, F. P. Bertolotti and D. S. Henningson “NOLOT-Non-Local Linear Stability Equations” FOI, FFA TN 1994-54 (1995)
- [2] A. Westin, A. Boiko, B. Klingmann, V. Kozlov and P. Alfredsson “Experiments on a boundary layer subjected to free stream turbulence. Part I. Boundary Layer structure and receptivity.” *J. Fluid Mech.* 281, 193(1994)
- [3] Drazin and Reid “Hydrodynamic Stability” Cambridge Univ. Press, 1981
- [4] D. W. Wundrow and M. E. Goldstein “Effect on a laminar boundary layer of small-amplitude streamwise vorticity in the upstream flow.” *J. Fluid Mech.* 426, 29(2001)
- [5] F. P. Bertolotti, Th. Herbert and P. R. Spalart “Linear and nonlinear stability of the Blasius boundary Layer” *J. Fluid Mech.* 98, 441(1992)
- [6] H. Fasel and U. Konzelmann “Non-parallel stability of a flat-plate boundary layer using the complete Navier-Stokes equations” *J. Fluid Mech.* 311, 221(1990)
- [7] H. Schlichting and K. Gersten “Boundary Layer Theory” 8th ed, Springer-Verlag, Berlin Heidelberg, 2000
- [8] J. Pralits, C. Airiau, A. Hanifi and D. S. Henningson “Sensitivity Analysis Using Adjoint Parabolized Stability Equations for Compressible Flows” *Flow, Turbulence and Combustion* 65, 321 (2000)
- [9] L. Brandt and C. Cossu “Stabilization of Tollmien-Schlichting waves by finite amplitude optimal streaks in the Blasius boundary layer” *Phys. Fluids* 14, L57(2002)
- [10] L. Brandt, C. Cossu, J. H. M. Fransson and A. Talamelli “Experimental and theoretical investigation of the non-modal growth of steady streaks in a flat boundary layer” *Phys. Fluids* 17, 054110(2005)
- [11] L. Brandt and C. Cossu “On Tollmien-Schlichting-like waves in streaky boundary layers” *Eur. J. Mech. B/Fluids* 23, 815(2004)
- [12] L. Brandt, C. Cossu, J. H. M. Fransson and A. Talamelli “Experimental study of the stabilization of Tollmien-Schlichting waves by finite amplitude streaks” *Phys. Fluids* 17, 054110(2005)
- [13] L. Brandt, C. Cossu, J. H. M. Fransson and A. Talamelli “Delaying transition to Turbulence by a Passive Mechanism” Submitted to *Phys. Rev. Letters* (2006)
- [14] M. N. Kogan and M. V. Ustinov “Boundary Layer Stabilization by “Artificial Turbulence”” *Fluid Dynamics* 38, 571(2003)

- [15] O. Levin and D. S. Henningson “Exponential vs Algebraic Growth and Transition Prediction in Boundary Layer Flow” *Flow, Turbulence and Combustion* 70, 183 (2003)
- [16] P. Andersson, M. Berggren and D. S. Henningson “Optimal disturbances and bypass transition in boundary layers” *Phys. Fluids* 11, 134(1999)
- [17] P. Andersson, L. Brandt, A. Bottareo and D. Henningson “On the breakdown of boundary layer streaks.” *J. Fluid Mech.* 482, 29(2001)
- [18] P. Andersson, D. Henningson and A. Hanifi “On the stabilization procedure for the parabolic equations.” *J. Fluid Mech.* 482, 29(2001)
- [19] P. J. Schmid and D.S Henningson “Stability and Transition in Shear Flows” Springer-Verlag, New York, 2001
- [20] Th. Herbert “Parabolized Stability Equations” *Agard Report* 793, 4-1(1994)

FOI is an assignment-based authority under the Ministry of Defence. The core activities are research, method and technology development, as well as studies for the use of defence and security. The organization employs around 1350 people of whom around 950 are researchers. This makes FOI the largest research institute in Sweden. FOI provides its customers with leading expertise in a large number of fields such as security-policy studies and analyses in defence and security, assessment of different types of threats, systems for control and management of crises, protection against and management of hazardous substances, IT-security and the potential of new sensors.



FOI
Swedish Defence Research Agency
SE-164 90 STOCKHOLM

Tel: +46 8 5550 3000
Fax: +46 8 5550 3100

www.foi.se